Original electric-vertex formulation of the symmetric eight-vertex model on the square lattice is fully nonuniversal

Roman Krčmár and Ladislav Šamaj

Institute of Physics, Slovak Academy of Sciences, Dúbravská cesta 9, SK-84511 Bratislava, Slovakia

The partition function of the symmetric (zero electric field) eight-vertex model on a square lattice can be formulated either in the original "electric" vertex format or in an equivalent "magnetic" Ising-spin format. In this paper, both electric and magnetic versions of the model are studied numerically by using the corner transfer matrix renormalization-group method which provides reliable data. The emphasis is put on the calculation of four specific critical exponents, related by two scaling relations, and of the central charge. The numerical method is first tested in the magnetic format, the obtained dependencies of critical exponents on the model's parameters agree with Baxter's exact solution, and weak universality is confirmed within the accuracy of the method due to the finite size of the system. In particular, the critical exponents η and δ are constant as required by weak universality. On the other hand, in the electric format, analytic formulas based on the scaling relations are derived for the critical exponents η_e and δ_e which agree with our numerical data. These exponents depend on the model's parameters which is evidence for the full nonuniversality of the symmetric eight-vertex model in the original electric formulation.

I. INTRODUCTION

The two-dimensional (2D) eight-vertex model on the square lattice was proposed as a generalization of ice-type systems in 1970 [1,2]. Its symmetric (zero electric field) version was solved by using the idea of commuting transfer matrices and the Yang-Baxter equation for the scattering matrix as the consistency condition [3–6]. This became a basis for generating and solving systematically integrable models within the so-called "quantum inverse-scattering method" (QISM) [7,8]; see Refs. [9,10].

The partition function of the original "electric" eight-vertex formulation can be mapped onto the partition function of a "magnetic" Ising model on the dual square lattice with plaquette interactions [11,12]. The exact magnetic critical exponents of the symmetric eight-vertex model depend continuously on the model's parameters [6]. This violates the universality hypothesis which states that critical exponents of a statistical system depend only on the symmetry of microscopic state variables and the spatial dimensionality of the system [13]. Suzuki [14] formulated the singularities of statistical quantities near the critical point not in terms of the usual temperature difference, but in terms of the inverse correlation length which also goes to zero when approaching the critical point. The rescaled critical exponents are universal; this phenomenon is known as "weak universality." The necessary condition for weak universality is the constant value of critical exponents defined just at the critical point, namely η and δ, since the freedom in the definition of deviation from the critical point has no effect on these exponents.

Kadanoff and Wegner [12] suggested that the variation of critical indices is due to the special hidden symmetries of the zero-field eight-vertex model. If an external field is applied, they argued that the magnetic exponents should be constant and equivalent to those of the standard 2D Ising model; see also Ref. [6]. This conjecture was supported by renormalization-group calculations [15–17]. Recently, the conjecture was confirmed numerically, except for two specific "semisymmetric" combinations of vertical and horizontal electric fields for which the model still exhibits weak universality [18].

Historically, the next weakly universal Ashkin-Teller model [19–22] is in fact related to the eight-vertex model [16]. Weak universality appears also in interacting dimers [23], frustrated spins [24,25], quantum phase transitions [26], models of percolation [27], etc. There are indications that both universality and weak universality are violated in the symmetric 16-vertex model on the 2D square and three-dimensional (3D) diamond lattices [28,29], Ising spin glasses [30], frustrated spin models [31], experimental measurements on composite materials [32,33], etc.

The six-vertex model is a simplified ice-type version of the eight-vertex model with certain vertex weights equal to zero. This model, represented as the quantum Heisenberg XXZ spin-$\frac{1}{2}$ chain, is related to many other systems like supersymmetric spin chains [34–39], 2D loop and tilling models [40–42], the random-cluster model of Fortuin and Kasteleyn [43–45], the restricted solid-on-solid model [46,47] and classical 2D Potts models [48,49]. The relations of the six-vertex model to these models have a precise meaning within Temperley-Lieb algebra representation theory [50]. Although all partition functions of the related models are equal, the content of critical exponents is only partially overlapping.

The polarization is an order parameter in the symmetric eight-vertex model. The corresponding critical exponent β_e, which depends on the model's parameters, is the only exactly known electric exponent [6]. The restriction to the six-vertex model and the related XXZ spin chain provides additional information about electric critical exponents. Using previous

results about the arrow correlation length exponent for the six-vertex model [51], Luther and Peschel [52] have shown that the arrow correlation function is the same as the transverse spin correlation of the Heisenberg XXZ model. Using a generalization of the Jordan-Wigner transformation for spin operators, they were able to calculate the asymptotic behavior of spin correlation functions for a continuum generalization of the spin-$\frac{1}{2}$ XXZ chain and suggested a formula for indices γ_e and η_e. The analytical predictions for the electric critical indices was verified well numerically by using the Trotter approximation [53]. The only numerical complication concerns the isotropic XXX antiferromagnetic chain where a multiplicative logarithmic correction for the correlation function exists; for a controversial discussion about this topic see Refs. [54–56]. A density-matrix renormalization-group study [57] improved the previous calculations of the logarithmic correction.

The aim of the present paper is to study numerically both magnetic and electric critical exponents of the symmetric eight-vertex model. To achieve a high accuracy, we apply the corner transfer matrix renormalization-group (CTMRG) method, based on the renormalization of the density matrix [58–61]. Four critical exponents which fulfill two scaling relations and the central charge are calculated in both magnetic and electric formats. The CTMRG method is first tested on the magnetic version of the symmetric eight-vertex model; the obtained dependence of magnetic critical exponents on the model's parameters is in good agreement with Baxter's exact solution and weak universality is verified. In particular, the critical exponents η and δ are constant, as required by weak universality. On the other hand, in the electric format, analytic formulas based on the scaling relations are derived for the critical exponents η_e and δ_e which agree with our numerical data. These exponent depends on the model's parameters which is evidence that both universality and weak universality are violated, i.e., the original electric formulation of the eight-vertex model is fully nonuniversal. Thus the equivalence of the electric and magnetic partition functions does not imply the same critical properties of the two model versions.

The paper is organized as follows. In Sec. II, we summarize basic facts about the symmetric eight-vertex model on the square lattice. These facts include the mapping onto the Ising model with plaquette interactions, definitions of critical exponents of interest, and of their scaling relations and the exact results of Baxter. In Sec. III, we review briefly the CTMRG numerical method and the evaluation techniques of magnetic and electric critical exponents. The numerical method is first tested on magnetic critical exponents in Sec. IV; their dependencies on the model's parameters agree with Baxter's values and the phenomenon of weak universality is checked within the accuracy of the method due to the finite size of the system. The numerical results for electric counterparts of critical exponents, presented in Sec. V, confirm clearly that the symmetric eight-vertex model is fully nonuniversal in its original vertex format. Section VI brings a brief recapitulation.

II. BASIC FACTS ABOUT THE SYMMETRIC EIGHT-VERTEX MODEL

In vertex models, one attaches to each lattice edge local two-state variables, say arrows directing to one of the two
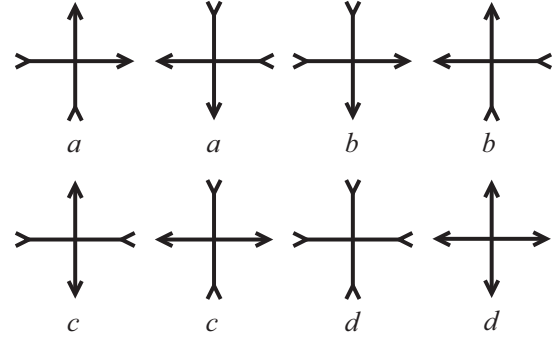

FIG. 1. Admissible configurations of the eight-vertex model, with the corresponding notation of the Boltzmann vertex weight.

vertices joined by the edge; the arrows can be interpreted as electric dipoles. In the eight-vertex model, each vertex configuration of edge states satisfies the rule that only an even (0, 2, or 4) number of arrows point toward the vertex. From among $2^4 = 16$ possible vertex configurations just eight ones fulfill this rule; the admissible configurations of arrows together with the corresponding Boltzmann vertex weights are presented in Fig. 1. In the symmetric version of the eight-vertex model considered here, the Boltzmann weight of a vertex configuration is invariant with respect to the reversal of all arrows incident to a vertex which corresponds to zero electric fields acting on dipole arrows. The Boltzmann vertex weights can be formally expressed in terms of local energies as follows:

$$a = C \exp(-\epsilon_a/T), \quad b = C \exp(-\epsilon_b/T),$$
$$c = C \exp(-\epsilon_c/T), \quad d = C \exp(-\epsilon_d/T), \tag{2.1}$$

where T is the temperature (in units of $k_B = 1$) and the value of the prefactor C is irrelevant. The partition function is defined by

$$Z_{8V}(T) = \sum \prod (\text{weights}), \tag{2.2}$$

where the summation goes over all possible edge configurations on the lattice and, for a given configuration, the product is taken over all vertex weights.

A. Mapping onto the Ising model

The symmetric eight-vertex model on the square lattice can be mapped onto its Ising counterpart defined on the dual (also square) lattice [11,12]. We assign $+1$ to the up or right arrows and -1 to the down or left arrows. A state configuration ϕ, χ, τ, κ ($\phi = \pm 1$, $\chi = \pm 1$, etc.) of incident edges is depicted in Fig. 2. The eight-vertex rule is equivalent to the constraint

$$\phi\chi\tau\kappa = 1. \tag{2.3}$$

The Ising spin variables on the dual square $\sigma_1, \sigma_2, \sigma_3, \sigma_4$ ($\sigma_1 = \pm 1$, $\sigma_2 = \pm 1$, etc.) are related to the vertex edge variables at the bond intersections as follows:

$$\phi = \sigma_1\sigma_2, \quad \chi = \sigma_3\sigma_4, \quad \tau = \sigma_1\sigma_3, \quad \kappa = \sigma_2\sigma_4. \tag{2.4}$$

Due to the equality $\phi\chi\tau\kappa = \sigma_1^2\sigma_2^2\sigma_3^2\sigma_4^2$ the eight-vertex requirement (2.3) is automatically fulfilled. Note that the spin-flip transformation $\sigma_i \rightarrow -\sigma_i$ for all $i = 1,2,3,4$ leaves the actual values of vertex states unchanged.
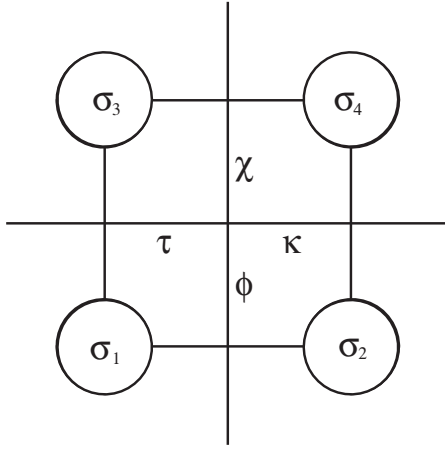
FIG. 2. Mapping from the electric-vertex formulation with edge states ϕ, χ, τ, κ to the magnetic Ising representation with site spin variables $\sigma_1, \sigma_2, \sigma_3, \sigma_4$.

The Ising Hamiltonian can be written as

$$H_{\mathrm{I}} = \sum_{\mathrm{plaq}} H_{\mathrm{plaq}}, \qquad (2.5)$$

where each square plaquette Hamiltonian H_{plaq} involves interactions of four spins $\sigma_1, \sigma_2, \sigma_3, \sigma_4 = \pm 1$ as depicted in Fig. 2. The plaquette Hamiltonian involves diagonal and four-spin interactions,

$$-H_{\mathrm{plaq}} = J\sigma_2\sigma_3 + J'\sigma_1\sigma_4 + J''\sigma_1\sigma_2\sigma_3\sigma_4. \qquad (2.6)$$

It exhibits the spin-flip symmetry $\sigma_i \to -\sigma_i$ $(i = 1,2,3,4)$.

The partition function of the eight-vertex model (2.2) and the one of the Ising model

$$Z_{\mathrm{I}}(T) = \sum_{\{\sigma\}} \exp(-H_{\mathrm{I}}/T) \qquad (2.7)$$

are equivalent,

$$Z_{\mathrm{I}}(T) = 2 Z_{8\mathrm{V}}(T), \qquad (2.8)$$

if the Boltzmann vertex weights are expressed in terms of the Ising interactions in the following way [6]:

$$
\begin{aligned}
a &= C \exp[(J + J' + J'')/T], \\
b &= C \exp[(-J - J' + J'')/T], \\
c &= C \exp[(-J + J' - J'')/T], \\
d &= C \exp[(J - J' - J'')/T].
\end{aligned}
\qquad (2.9)
$$

The Boltzmann vertex weight $w(\tau, \phi | \chi, \kappa)$, corresponding to the configuration of the edge state in Fig. 2, which is constrained by (2.3), is expressible in terms of Ising couplings as follows:

$$w(\tau, \phi | \chi, \kappa) = C \exp[(J\phi\tau + J'\chi\tau + J''\phi\chi)/T]. \qquad (2.10)$$

In terms of the free energy F defined as $-F/T = \ln Z$, the relation between the partition functions (2.8) is equivalent to

$$-F_{\mathrm{I}}(T)/T = \ln 2 - F_{8\mathrm{V}}(T)/T. \qquad (2.11)$$

For the internal energies defined by $U = -T^2 \partial(F/T)\partial T$, it holds that

$$U_{\mathrm{I}}(T) = U_{8\mathrm{V}}(T). \qquad (2.12)$$

Since the Ising Hamiltonian H_{I} is invariant with respect to the spin-flip transformation $\sigma_i \to -\sigma_i$ at all lattice sites, the Ising magnetization

$$M = \langle \sigma \rangle \qquad (2.13)$$

($\langle \cdots \rangle$ means the thermodynamic average) is a good order parameter in the ferromagnetic phase.

For every state configuration of edges incident to each vertex, the constraints (2.3) and the Boltzmann weights (2.10) are invariant with respect to the transformation $\phi, \chi, \tau, \kappa \to -\phi, -\chi, -\tau, -\kappa$. The isotropic polarization,

$$P = \langle \phi \rangle, \qquad (2.14)$$

is therefore a legitimate order parameter as well. Note that due to the relations between the arrow and spin variables (2.4), the polarization is equal to the correlation function of nearest-neighbor Ising spins.

B. Magnetic format: Exact results

The symmetric eight-vertex model has five phases [6]. We shall restrict ourselves to the ferroelectric-A phase defined by the inequality $a > b + c + d$ and the disordered phase in the region $a, b, c, d < (a + b + c + d)/2$. The second-order transition between these phases takes place at the hypersurface

$$a_c = b_c + c_c + d_c, \qquad (2.15)$$

where the c subscript means evaluated at the critical temperature T_c. Note that our vertex weights do not belong to the "principal regime" defined by the inequality $c > a + b + d$ (see Sec. 10.7 of Ref. [6]), so certain formulas in [6] written for vertex weights in the principal regime must be adapted to our case.

In general, only two critical exponents are independent and all other exponents can be expressed in terms of them by using scaling relations [6]. Here, we shall concentrate on four critical exponents.

Let us consider a small temperature deviation from the critical point $\Delta T = T - T_c$. For $\Delta T \to 0^-$, the spontaneous magnetization M behaves as

$$M \propto (-\Delta T)^\beta \qquad (2.16)$$

which defines the critical index β.

The pair spin-spin correlation function at distance r, $G(\mathbf{r}) = \langle \sigma_0 \sigma_{\mathbf{r}} \rangle$, has in two dimensions the large-distance asymptotic form

$$G(r) \propto \frac{1}{r^\eta} \exp(-r/\xi), \qquad (2.17)$$

where ξ is the correlation length. Approaching the critical point, the correlation length diverges as

$$\xi \underset{\Delta T \to 0^+}{\propto} \frac{1}{(\Delta T)^\nu}, \qquad \xi \underset{\Delta T \to 0^-}{\propto} \frac{1}{(-\Delta T)^{\nu'}}, \qquad (2.18)$$

where the critical exponents ν and ν' are in fact identical. Just at the critical point, where $\xi \to \infty$, the exponential short-range

decay of the correlation function (2.17) becomes long ranged,

$$G(r) \propto \frac{1}{r^\eta}, \qquad T = T_c, \tag{2.19}$$

which defines the exponent η.

Let us apply to the spin system an external magnetic field H, so that the Ising Hamiltonian can be written as

$$H_\mathrm{I} = \sum_\mathrm{plaq} H_\mathrm{plaq} - H \sum_i \sigma_i. \tag{2.20}$$

The critical point corresponds to $T = T_c$ and $H = 0$. At $T = T_c$ and for small H, the Ising magnetization $M(H)$ exhibits the singular behavior of type

$$M(H) \propto H^{1/\delta}, \qquad T = T_c, \tag{2.21}$$

which defines the critical exponent δ.

The von Neumann entropy is defined by

$$S_\mathrm{N} = -\mathrm{Tr}\,\rho \ln \rho, \tag{2.22}$$

where ρ is the density matrix of the Ising model defined below. At the critical point, the entropy grows with the size L of the system as [62,63]

$$S_\mathrm{N} \sim \frac{c}{6} \ln L, \qquad T = T_c, \tag{2.23}$$

where c is the central charge. It holds that $c = 1$ for the weakly universal symmetric eight-vertex model [6]. We recall that $c = 1/2$ for the universal 2D Ising model.

In two dimensions, the four exponents of interest fulfill two scaling relations [6],

$$\eta = 2\frac{\beta}{\nu}, \qquad \delta = \frac{4}{\eta} - 1. \tag{2.24}$$

According to the exact Baxter's solution of the symmetric eight-vertex model, the exponents β and ν, whose definition requires us to introduce the small temperature deviation ΔT, are given by [6]

$$\beta = \frac{\pi}{16\mu}, \qquad \nu = \frac{\pi}{2\mu}, \tag{2.25}$$

where the auxiliary parameter

$$\mu = 2 \arctan\left(\sqrt{\frac{a_c b_c}{c_c d_c}}\right) = 2 \arctan(e^{2J''/T_c}). \tag{2.26}$$

If $J'' = 0$, when the system splits into two independent Ising lattices with nearest-neighbor couplings J and J', we have $\mu = \pi/2$ and Eq. (2.25) gives the standard 2D Ising exponents

$$\beta_\mathrm{I} = \frac{1}{8}, \qquad \nu_\mathrm{I} = 1. \tag{2.27}$$

Suzuki's concept of weak universality [14] explains the dependence of the critical exponents (2.25) on J'' by the ambiguity in the definition of the deviation from the critical point. If one considers the inverse correlation length $\xi^{-1} \propto (T_c - T)^\nu$ with $T \to T_c^-$ instead of the temperature difference $T_c - T$, the new (rescaled) critical exponent

$$\hat{\beta} \equiv \frac{\beta}{\nu} = \frac{1}{8} \tag{2.28}$$

becomes universal. According to the definitions (2.19) and (2.21), the exponents η and δ are defined just at the critical temperature and as such do not depend on the definition of the deviation from the critical temperature. Therefore η and δ must be constant in a weakly universal theory and this fact is confirmed by Baxter's result,

$$\eta = \tfrac{1}{4}, \qquad \delta = 15, \tag{2.29}$$

i.e., $\eta = \eta_\mathrm{I}$ and $\delta = \delta_\mathrm{I}$. The scaling relations (2.24) evidently holds for the exponents (2.25) and (2.29).

C. Electric format: Exact results

As concerns the electric format, the only exactly known critical exponent [6]

$$\beta_\mathrm{e} = \frac{\pi - \mu}{4\mu}, \tag{2.30}$$

with μ defined by Eq. (2.26), describes the singular behavior of the spontaneous polarization near the critical point,

$$P \propto (-\Delta T)^{\beta_\mathrm{e}}. \tag{2.31}$$

In order to distinguish between magnetic and electric exponents, we add the subscript "e" to the latter.

In analogy with the magnetic system, we introduce the pair arrow-arrow correlation function at distance r, $G_\mathrm{e}(\mathbf{r}) = \langle \phi_\mathbf{0} \phi_\mathbf{r} \rangle$. In two dimensions, it exhibits the large-distance behavior of type

$$G_\mathrm{e}(r) \propto \frac{1}{r^{\eta_\mathrm{e}}} \exp(-r/\xi_\mathrm{e}). \tag{2.32}$$

Close to the critical point, the correlation length ξ_e diverges as

$$\xi_\mathrm{e} \underset{\Delta T \to 0^+}{\propto} \frac{1}{(\Delta T)^{\nu_\mathrm{e}}}, \qquad \xi_\mathrm{e} \underset{\Delta T \to 0^-}{\propto} \frac{1}{(-\Delta T)^{\nu_\mathrm{e}'}}, \tag{2.33}$$

where $\nu_\mathrm{e} = \nu_\mathrm{e}'$. At the critical point,

$$G(r) \propto \frac{1}{r^{\eta_\mathrm{e}}}, \qquad T = T_c. \tag{2.34}$$

Let us apply an isotropic electric field $E_x = E_y = E$, so that the Hamiltonian changes by $-E \sum_{\langle i,j \rangle} \phi_{\langle i,j \rangle}$ where $\phi_{\langle i,j \rangle}$ is the state variable on the edge connecting nearest-neighbor sites i and j. The critical point corresponds to $T = T_c$ and $E = 0$. At $T = T_c$ and for small E, the polarization $P(E)$ behaves as

$$P(E) \propto E^{1/\delta_\mathrm{e}}, \qquad T = T_c, \tag{2.35}$$

which defines the electric exponent δ_e.

As in the magnetic format, the von Neumann entropy S_N^e is defined by (2.22) with ρ being the density matrix of the vertex model. At the critical point, the entropy grows with the system size L as

$$S_\mathrm{N}^\mathrm{e} \sim \frac{c_\mathrm{e}}{6} \ln L, \qquad T = T_c, \tag{2.36}$$

where c_e is the electric central charge.

The four electric critical exponents of interest fulfill the electric counterparts of scaling relations (2.24):

$$\eta_\mathrm{e} = 2\frac{\beta_\mathrm{e}}{\nu_\mathrm{e}}, \qquad \delta_\mathrm{e} = \frac{4}{\eta_\mathrm{e}} - 1. \tag{2.37}$$
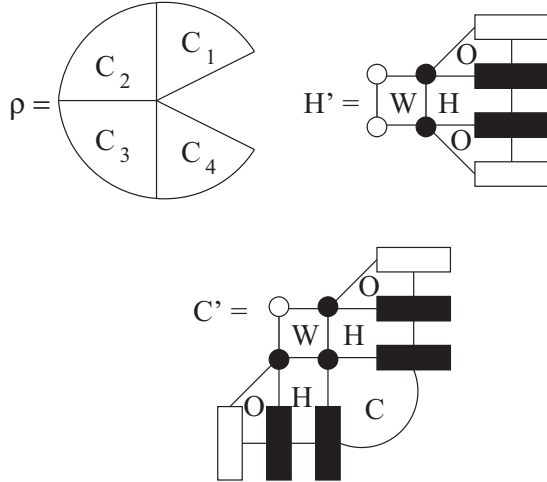
FIG. 3. The CTMRG renormalization process. The density matrix ρ is composed of four transfer matrices C_1, C_2, C_3, and C_4; each straight line represents L matrix site indices which are either fixed ("free" lines adjacent to C_1 and C_4) or summed out [common lines of pairs (C_1,C_2), (C_2,C_3), and (C_3,C_4)]. The expansion process of the corner transfer matrix C and the half-row transfer matrix H from the previous iteration, see text.

III. NUMERICAL METHOD

A. CTMRG approach

The CTMRG method [64,65] is based on Baxter's technique of corner transfer matrices [6]. Each quadrant of the square lattice with size $L \times L$ is represented by one of the corner transfer matrices $C_1, \ldots, C_4$ and the partition function $Z = \mathrm{Tr}(C_1 C_2 C_3 C_4)$. The density matrix is defined by $\rho = C_1 C_2 C_3 C_4$, see Fig. 3, so that $Z = \mathrm{Tr}\,\rho$. The number of degrees of freedom grows exponentially with L and the density matrix is used in the process of their reduction. Namely, degrees of freedom are iteratively projected to the space generated by the eigenvectors of the density matrix with the largest eigenvalues. The projector on this reduced space of dimension D will be denoted by O; the larger the truncation parameter D taken, the better is the precision of the results attained. In each iteration the linear size of the system is expanded from L to $L+2$ via the inclusion of the Boltzmann weight W of the basic plaquette cell (see Fig. 2). The expansion process transforms the corner transfer matrix C to C' and the half-row transfer matrix H to H' in the way represented schematically in Fig. 3. The empty boxes (circles) represent new multispin (spin) variables obtained after the renormalization which consists in the summation and O projection of multispin (spin) black boxes (circles) from the previous iteration. The fixed boundary conditions are used, with each spin at the boundary set to the value $\sigma = -1$. This choice ensures a quicker convergence of the method in the ordered phase.

Technically, one has to distinguish between two choices of vertex weights c and d.

The choice

$$c = d \qquad (3.1)$$

leads to the symmetric density matrix ρ. In the Ising representation (2.9), the choice (3.1) corresponds to the constraint

$J = J'$. The original formulation of CTMRG [64,65] requires that the density matrix ρ is symmetric. In that case we can return to the row-to-row transfer matrix $\mathcal{T}$ and denote by $|\psi_0^{(l)}\rangle$ and $|\psi_0^{(r)}\rangle$ its left and right eigenvectors corresponding to the largest eigenvalue, respectively. For the symmetric $\mathcal{T}$, we have the equality $|\psi_0^{(l)}\rangle = |\psi_0^{(r)}\rangle$. In the limit $L \to \infty$, the product of the corner matrices $C_1 C_2$ is expressible as $|\psi_0^{(l)}\rangle$ and $C_3 C_4$ as $\langle \psi_0^{(r)}|$, so that

$$\rho = \mathrm{Tr}\,|\psi_0^{(l)}\rangle\langle\psi_0^{(r)}|. \qquad (3.2)$$

Here, the trace is taken over common indices of the corner matrices C_2 and C_3; see Fig. 3.

If

$$c \neq d, \qquad (3.3)$$

it holds that $|\psi_0^{(l)}\rangle \neq |\psi_0^{(r)}\rangle$ and the density matrix is nonsymmetric. Within the Ising representation (2.9), this choice of vertex weights corresponds to the inequality $J \neq J'$. It can be shown [59,66] that the symmetrized density matrix

$$\rho = \tfrac{1}{2}\,\mathrm{Tr}\left(|\psi_0^{(l)}\rangle\langle\psi_0^{(l)}| + |\psi_0^{(r)}\rangle\langle\psi_0^{(r)}|\right) \qquad (3.4)$$

provides an optimal basis set which minimizes the distance of a trial vector in the reduced space (of dimension D) from the right and left eigenstates $|\psi_0^{(l)}\rangle$ and $|\psi_0^{(r)}\rangle$. This fact allows us to use the symmetrized density matrix (3.4) within the standard CTMRG [64,65] when treating the more complicated case (3.3). The only exception is the von Neumann entropy (2.22) for which the above approach does not work and therefore in this case we shall consider only the choice $c = d$ with the symmetric density matrix ρ.

B. Calculation of critical exponents

First we focus on the magnetic critical exponents ν, η, β, δ and the central charge c, and then on their electric counterparts.

1. Magnetic exponents

The critical magnetic exponent ν can be obtained from the dependence of the internal energy U_{I} on the linear size of the system L at the critical point [67],

$$U_{\mathrm{I}}(L) - U_{\mathrm{I}}(\infty) \propto L^{-2+1/\nu}, \qquad T = T_c. \qquad (3.5)$$

The effective (i.e., L-dependent) exponent ν^{eff} is calculated as the logarithmic derivative of the internal energy as follows:

$$\nu^{\mathrm{eff}}(L) = \left[3 + \frac{\partial}{\partial \ln L}\ln\left(\frac{\partial U_{\mathrm{I}}}{\partial L}\right)\right]^{-1}. \qquad (3.6)$$

If T is close to the critical T_c, the plot $\nu^{\mathrm{eff}}(L)$ either goes to 0 (in the ordered phase) or diverges (in the disordered phase) with increasing L. We can therefore determine the critical temperature T_c from the requirement that $\nu^{\mathrm{eff}}(L)$ goes to a finite nonzero value as $L \to \infty$, i.e.,

$$\lim_{L \to \infty} \nu^{\mathrm{eff}}(L) \to \nu, \qquad T = T_c, \qquad (3.7)$$

where $0 < \nu < \infty$ is the critical exponent we are searching for. For the model under consideration with the known critical manifold this procedure is not necessary, but we checked that it reproduces with a high precision the exact relation (2.15).

The magnetic index η follows from the L dependence of the magnetization at the critical point [67],

$$M \underset{L \to \infty}{\propto} L^{-\eta/2}, \qquad T = T_c. \tag{3.8}$$

The effective exponent η^{eff} is calculated as the logarithmic derivative of magnetization

$$\eta^{\text{eff}}(L) = -2\frac{\partial \ln M}{\partial \ln L}. \tag{3.9}$$

As before, $\eta = \lim_{L \to \infty} \eta^{\text{eff}}(L)$.

To calculate the magnetic exponent β, we make use of the T dependence of the spontaneous magnetization M close to the critical temperature T_c; see Eq. (2.16). The effective exponent β^{eff} is extracted via the logarithmic derivative

$$\beta^{\text{eff}}(T) = \frac{\partial \ln M}{\partial \ln(T_c - T)}. \tag{3.10}$$

In general, β^{eff} as a function of T has one extreme (maximum) at T^*, decays slowly for $T < T^*$ and drops abruptly for $T^* < T < T_c$, as a sign that the CTMRG method is inaccurate close to T_c. The extreme condition $\partial \beta^{\text{eff}}/\partial T|_{T=T^*} = 0$ indicates a weak dependence of β^{eff} on T close to T^*. This is why we take as the critical index β the maximal value of β^{eff}, $\beta = \beta^{\text{eff}}(T^*)$.

To obtain the magnetic exponent δ, we recall that the magnetization M behaves at the critical temperature $T = T_c$ according to the relation (2.21). The effective exponent δ^{eff} is calculated as follows:

$$\delta^{\text{eff}}(H) = \left(\frac{\partial \ln M}{\partial \ln H}\right)^{-1}. \tag{3.11}$$

In close analogy with the case of β^{eff}, δ^{eff} as a function of H has one extreme (minimum) at H^* and $\delta = \delta^{\text{eff}}(H^*)$.

As concerns the von Nemann entropy (2.22), at $T = T_c$ we define the effective central charge

$$c^{\text{eff}}(L) = 6\frac{\partial S_N}{\partial \ln L} \tag{3.12}$$

and $c = \lim_{L \to \infty} c^{\text{eff}}(L)$.

2. Electric exponents

Now we pass to the electric critical exponents. The critical index ν_e can be calculated from the electric counterpart of Eq. (3.5),

$$U_{8V}(L) - U_{8V}(\infty) \propto L^{-2+1/\nu_e}, \qquad T = T_c. \tag{3.13}$$

Choosing the equivalent boundary conditions, the relation between the Ising and vertex internal energies (2.12) can be adopted for any system size L,

$$U_I(T,L) = U_{8V}(T,L). \tag{3.14}$$

In view of relations (3.5) and (3.13), the corresponding magnetic and electric exponents coincide:

$$\nu_e = \nu. \tag{3.15}$$

The critical electric index η_e follows from the large-L dependence of the polarization at the critical point [67],

$$P \propto L^{-\eta_e/2}, \qquad T = T_c. \tag{3.16}$$

The effective exponent η_e^{eff} is calculated as

$$\eta_e^{\text{eff}}(L) = -2\frac{\partial \ln P}{\partial \ln L}. \tag{3.17}$$

Finally, $\eta_e = \lim_{L \to \infty} \eta_e^{\text{eff}}(L)$.

Taking into account that below the critical temperature the spontaneous polarization P behaves as

$$P \propto (T_c - T)^{\beta_e} \qquad \text{as } T \to T_c^-, \tag{3.18}$$

the effective exponent β_e^{eff} is retrieved via

$$\beta_e^{\text{eff}}(T) = \frac{\partial \ln P}{\partial \ln(T_c - T)}. \tag{3.19}$$

The critical index β_e corresponds to the maximal value of $\beta_e^{\text{eff}}(T)$ at $T = T^*$, $\beta_e = \beta_e^{\text{eff}}(T^*)$.

The electric exponent δ_e is defined by the singular dependence (2.35) of the polarization P at $T = T_c$, under weak electric field E. Defining the effective exponent δ_e^{eff} as

$$\delta_e^{\text{eff}}(E) = \left(\frac{\partial \ln P}{\partial \ln E}\right)^{-1}. \tag{3.20}$$

and denoting the minimum point of the plot $\delta_e^{\text{eff}}(E)$ as E^*, we have $\delta_e = \delta_e^{\text{eff}}(E^*)$.

Using the von Nemann entropy at $T = T_c$, we define the effective electric central charge as

$$c_e^{\text{eff}}(L) = 6\frac{\partial S_N^e}{\partial \ln L} \tag{3.21}$$

and $c_e = \lim_{L \to \infty} c_e^{\text{eff}}(L)$.

IV. NUMERICAL ANALYSIS OF MAGNETIC EXPONENTS

In all considered cases, for simplicity we fix the vertex energy $\epsilon_a = 0$, i.e., $a = a_c = 1$. The value of the critical temperature T_c is set to 1. In what follows, the truncation
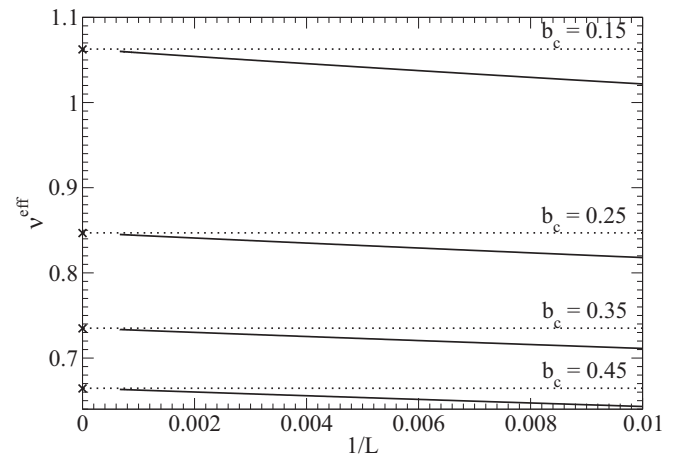

FIG. 4. The symmetric eight-vertex model with $c = d$: the dependence of the effective critical index ν^{eff} on the inverse system size $1/L$, for four values of the critical vertex weight $b_c = 0.15$, 0.25, 0.35, and 0.45. As $1/L$ goes to 0, the linear $a + b/L$ fittings of $\nu^{\text{eff}}(L)$ give the asymptotic ν values denoted by crosses. Baxter's exact values are represented by dotted lines.
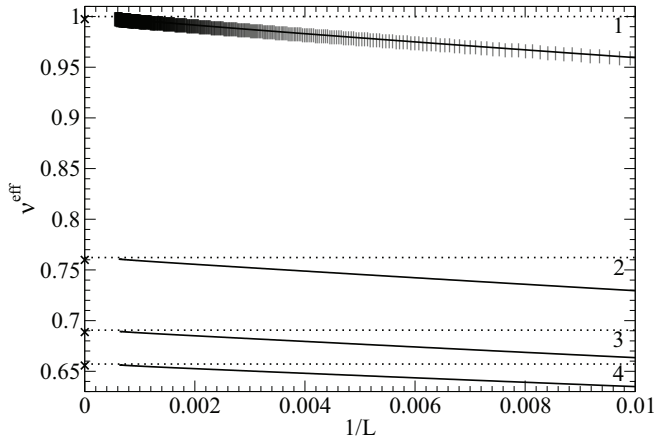
FIG. 5. The symmetric eight-vertex model with $c \neq d$: the dependence of ν^{eff} on $1/L$, for four choices of the critical vertex weights (4.2). The asymptotic ν values are denoted by crosses, Baxter's exact values are represented by dotted lines.

parameter $D = 1000$ in all L-dependent plots, while $D = 200$ in all dependencies of the effective exponents on the deviation from the critical temperature $\Delta T = T_c - T$ or the applied magnetic (electric) H (E) field. The critical hypersurface (2.15) of the ferroelectric-A phase is considered.

The symmetric eight-vertex model with $c = d$ is then defined by

$$b_c, \qquad c_c = \frac{1 - b_c}{2}. \tag{4.1}$$

The values of b_c under consideration are 0.15, 0.25, 0.35, and 0.45.

In the case of the symmetric eight-vertex model with $c \neq d$, we consider four choices of vertex weights:

$$
\begin{aligned}
1: \quad & b_c = 0.15, \quad c_c = 0.60, \quad d_c = 0.25, \\
2: \quad & b_c = 0.25, \quad c_c = 0.15, \quad d_c = 0.60, \\
3: \quad & b_c = 0.35, \quad c_c = 0.50, \quad d_c = 0.15, \\
4: \quad & b_c = 0.45, \quad c_c = 0.20, \quad d_c = 0.35.
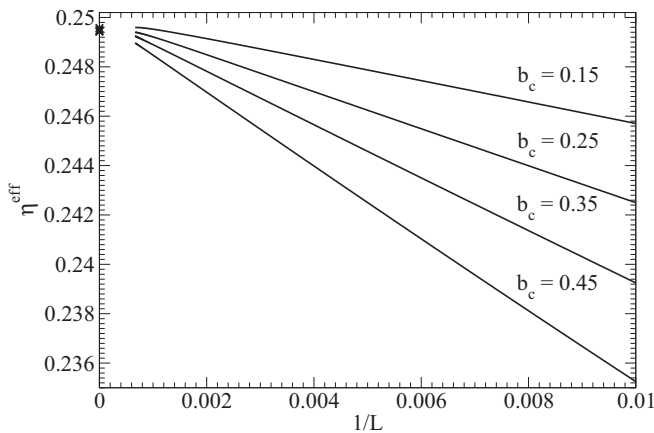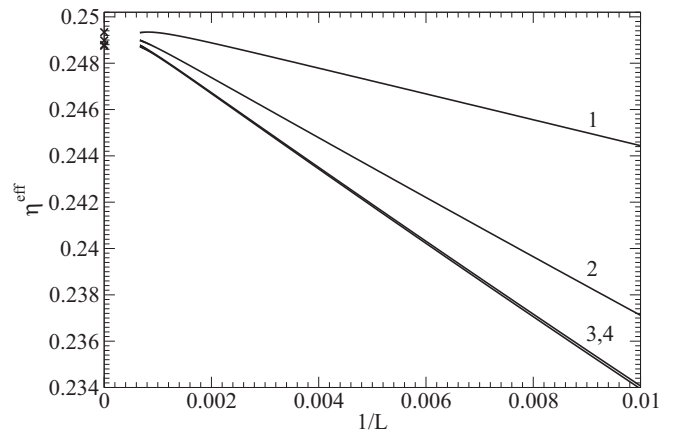\end{aligned}
\tag{4.2}
$$

FIG. 6. The symmetric eight-vertex model with $c = d$: the dependence of the effective critical index η^{eff} on the inverse system size $1/L$, for four values of the critical vertex weight $b_c = 0.15$, 0.25, 0.35, and 0.45. In all cases, as $1/L \to 0$, η^{eff} goes to 1/4.

FIG. 7. The symmetric eight-vertex model with $c \neq d$: the dependence of η^{eff} on $1/L$, for four choices of the critical vertex weights (4.2). In all cases, η^{eff} goes asymptotically to 1/4.

In this section, our numerical method is first tested within the framework of the magnetic formulation, with the known Baxter's values of critical exponents. The obtained numerical results will be first presented in figures to document visually their accuracy, then the numerical values obtained via asymptotic fits will be tabulated and compared with the exact values in Table I at the end of this section.

The effective exponent ν^{eff} as a function of the inverse system size $1/L$ is pictured in Fig. 4 for $c = d$ and in Fig. 5 for $c \neq d$. As $1/L$ goes to 0, the linear $a + b/L$ fittings of $\nu^{\mathrm{eff}}(L)$ give the asymptotic ν values denoted by crosses which are close to the Baxter's exact values of ν represented by the horizontal dotted lines. The number of individual values of L used in the numerical calculation is documented by vertical segments in Fig. 5 on the plot corresponding to the choice 1 of vertex weights; we recall that the difference between segments corresponds to the increase of L by 2. We see that as $1/L \to 0$

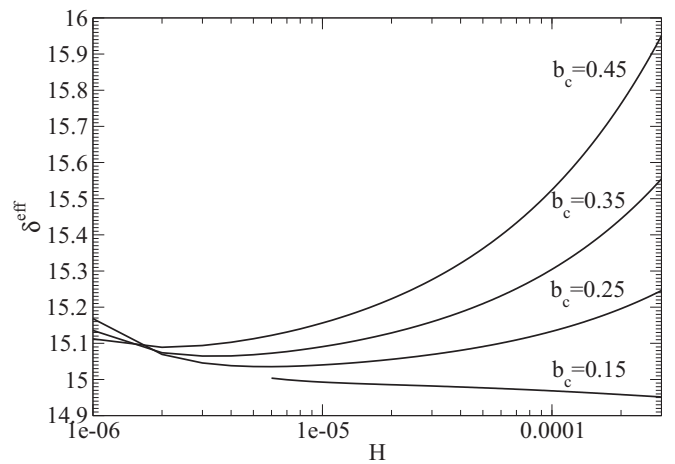FIG. 8. The symmetric eight-vertex model with $c = d$: the dependence of the effective critical exponent δ^{eff} on the applied magnetic field H, for four values of the critical vertex weight $b_c = 0.15$, 0.25, 0.35, and 0.45. The actual δ values, identified with the minimum points of the plots, are close to the exact Baxter's result, $\delta = 15$.
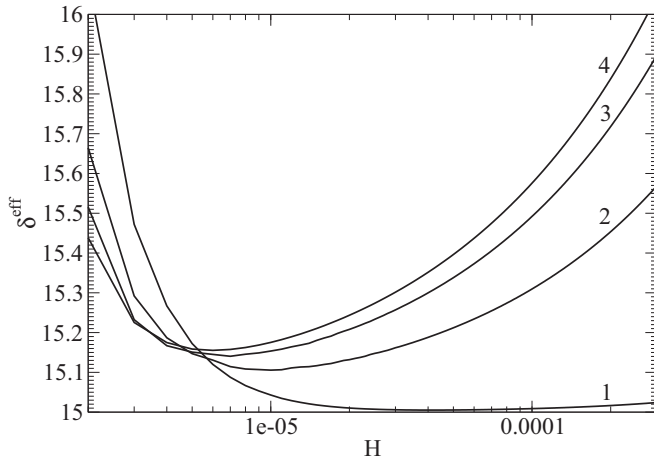
FIG. 9. The symmetric eight-vertex model with $c \neq d$: the dependence of δ^{eff} on the magnetic field H, for four choices of the critical vertex weights (4.2).

the point set is quasicontinuous. Since $\ln(L+2) - \ln L \sim 2/L$ for large L, the discrete evaluation of the derivative with respect to $\ln L$ is accurate.

The dependence of the effective exponent η^{eff} on the inverse system size $1/L$ is presented in Fig. 6 for $c = d$ and in Fig. 7 for $c \neq d$. As L increases, all curves converge to the Ising value $\eta = 1/4$ as it should be for a weakly universal critical theory. Note that the curves corresponding to choices 3 and 4 in Fig. 7 are indistinguishable in the present zoom.

In the logarithmic scale, the plots of the effective exponent δ^{eff} versus the applied magnetic field H are presented in Fig. 8 for $c = d$ and in Fig. 9 for $c \neq d$. The actual δ values are identified with the minimum points of the plots. They are close to the Baxter's constant prediction $\delta = 15$. The only exception
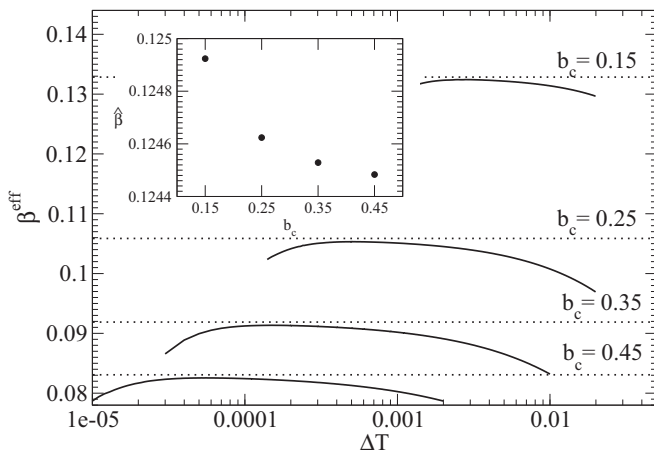

FIG. 10. The symmetric eight-vertex model with $c = d$: the effective exponent β^{eff} vs the deviation from the critical point $\Delta T = T_c - T$, for four values of the critical vertex weight $b_c = 0.15$, 0.25, 0.35, and 0.45. The β values are identified with the maximum points of the plots, Baxter's exact values are represented by dotted lines. The inset documents an almost constant dependence of the rescaled exponent $\hat{\beta} = \beta/\nu \sim 1/8$ on b_c.

is the plot for $b_c = 0.15$ which does not exhibit a minimum and therefore we fitted the original dependence (2.21).

In the logarithmic scale, the numerical results for the effective exponent β^{eff} as the function of the deviation from the critical temperature ΔT are presented in Fig. 10 for $c = d$ and in Fig. 11 for $c \neq d$. The plots of $\beta^{\text{eff}}(\Delta T)$ exhibit maxima values close to Baxter's exact results for β (dotted lines) as it should be. The insets of the figures show the model's dependence of the exponent ratio $\hat{\beta} = \beta/\nu$. In spite of a slight dispersion of the results, $\hat{\beta}$ is close to the Ising value $\beta_{\text{I}} = 1/8$, in agreement with the concept of weak universality.

For the vertex weights $c = d$, the magnetic effective central charge c^{eff} is presented as a function of the inverse system size $1/L$ in Fig. 12. For all four values of the critical vertex weight $b_c = 0.15$, 0.25, 0.35, and 0.45, as $1/L \to 0$ the plots tend to the value $c = 1$ which is the central charge of the weakly universal symmetric eight-vertex model [6].
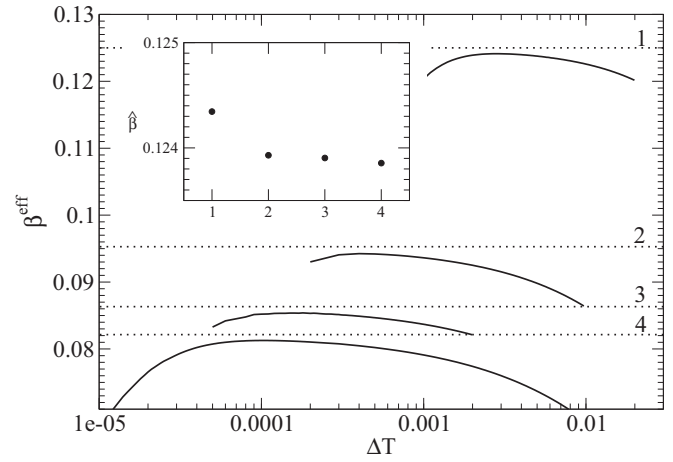

FIG. 11. The symmetric eight-vertex model with $c \neq d$: the dependence of β^{eff} on ΔT for four choices of the critical vertex weights (4.2). Baxter's exact values are represented by dotted lines. The inset shows the dependence of $\hat{\beta}$ on b_c.
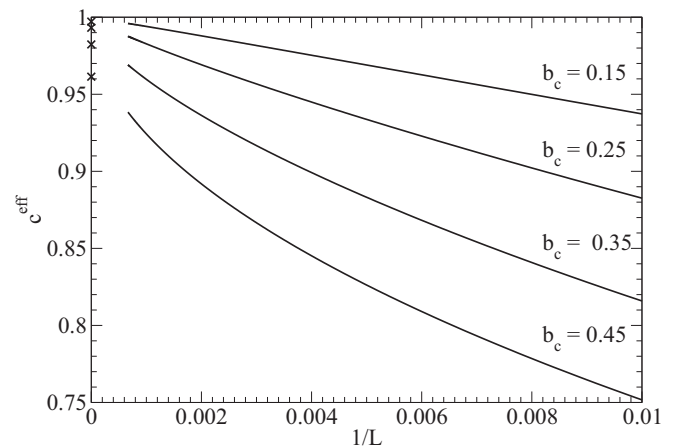

FIG. 12. The symmetric eight-vertex model with $c = d$: the dependence of the magnetic effective central charge c^{eff} on $1/L$, for four values of the critical vertex weight $b_c = 0.15$, 0.25, 0.35, and 0.45. As $1/L \to 0$, all curves tend to the central charge $c = 1$.

TABLE I. Numerical data for the magnetic exponents and central charge obtained from Figs. 4–12 and compared with the Baxter's exact results.

Fig. 4:	$b_c = 0.15$	$\nu^{num} = 1.0624$	$\nu^{exact} = 1.0628$
	$= 0.25$	$= 0.8468$	$= 0.8470$
	$= 0.35$	$= 0.7349$	$= 0.7351$
	$= 0.45$	$= 0.6643$	$= 0.6646$
Fig. 5:	1	$\nu^{num} = 0.9975$	$\nu^{exact} = 1.0000$
	2	$= 0.7599$	$= 0.7622$
	3	$= 0.6887$	$= 0.6906$
	4	$= 0.6557$	$= 0.6572$
Fig. 6:	$b_c = 0.15$	$\eta^{num} = 0.2496$	$\eta^{exact} = 1/4$
	$= 0.25$	$= 0.2494$	$= 1/4$
	$= 0.35$	$= 0.2495$	$= 1/4$
	$= 0.45$	$= 0.2494$	$= 1/4$
Fig. 7:	1	$\eta^{num} = 0.2493$	$\eta^{exact} = 1/4$
	2	$= 0.2490$	$= 1/4$
	3	$= 0.2488$	$= 1/4$
	4	$= 0.2487$	$= 1/4$
Fig. 8:	$b_c = 0.15$	$\delta^{num} = 15.0355$	$\delta^{exact} = 15$
	$= 0.25$	$= 15.0648$	$= 15$
	$= 0.35$	$= 15.0891$	$= 15$
	$= 0.45$	$= 14.9811$	$= 15$
Fig. 9:	1	$\delta^{num} = 15.0051$	$\delta^{exact} = 15$
	2	$= 15.1055$	$= 15$
	3	$= 15.1404$	$= 15$
	4	$= 15.1554$	$= 15$
Fig. 10:	$b_c = 0.15$	$\beta^{num} = 0.1324$	$\beta^{exact} = 0.1328$
	$= 0.25$	$= 0.1053$	$= 0.1059$
	$= 0.35$	$= 0.0913$	$= 0.0919$
	$= 0.45$	$= 0.0826$	$= 0.0831$
Fig. 11:	1	$\beta^{num} = 0.1241$	$\beta^{exact} = 0.1250$
	2	$= 0.0942$	$= 0.0953$
	3	$= 0.0854$	$= 0.0863$
	4	$= 0.0813$	$= 0.0821$
Fig. 12:	$b_c = 0.15$	$c^{num} = 0.9972$	$c^{exact} = 1$
	$= 0.25$	$= 0.9932$	$= 1$
	$= 0.35$	$= 0.9823$	$= 1$
	$= 0.45$	$= 0.9614$	$= 1$

Numerical data for the magnetic exponents obtained from Figs. 4–12 are tabulated in Table I. The comparison with Baxter's exact results confirms a high precision of our numerical results.

V. NUMERICAL ANALYSIS OF ELECTRIC EXPONENTS

In the logarithmic scale, the numerical results for the effective exponent β_e^{eff} as the function of the deviation from the critical temperature ΔT are presented in Fig. 13 for $c = d$ and in Fig. 14 for $c \neq d$. The plots of $\beta^{eff}(\Delta T)$ exhibit maxima close to Baxter's exact result for β_e (2.30) (horizontal dotted lines). This fact confirms the adequacy of our numerical results also in the electric format.

Let us combine Baxter's exact result for the electric exponent β_e (2.30) with the equality between magnetic and electric ν indices (3.15) and the scaling relations (2.37). The exponents
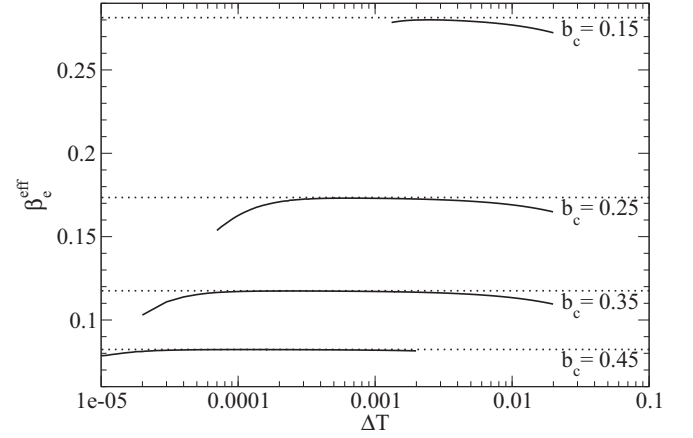

FIG. 13. The symmetric eight-vertex model with $c = d$: the electric effective exponent β_e^{eff} vs the deviation from the critical point $\Delta T = T_c - T$, for four values of the critical vertex weight $b_c = 0.15, 0.25, 0.35,$ and 0.45. The β_e values are identified with the maximum points of the plots, Baxter's exact values are represented by dotted lines.

η_e and δ_e are then given by

$$\eta_e = 1 - \frac{\mu}{\pi}, \qquad \delta_e = \frac{3\pi + \mu}{\pi - \mu}. \qquad (5.1)$$

As was explained before, the dependence of the electric exponents η_e and δ_e, defined just at the critical temperature, on a model's parameters means that the original electric version of the symmetric eight-vertex model cannot be weakly universal, but it is fully nonuniversal.

The plot of the effective exponent η_e^{eff} versus the inverse system size $1/L$ is pictured in Fig. 15 for $c = d$ and in Fig. 16 for $c \neq d$. As L increases, the curves converge to the asymptotic values (crosses) which are in agreement with our suggested formula (5.1).

In the logarithmic scale, the plots of the effective exponent δ_e^{eff} versus the applied electric field E are pictured in Fig. 17 for $c = d$ and in Fig. 18 for $c \neq d$. Note the shallowness of the

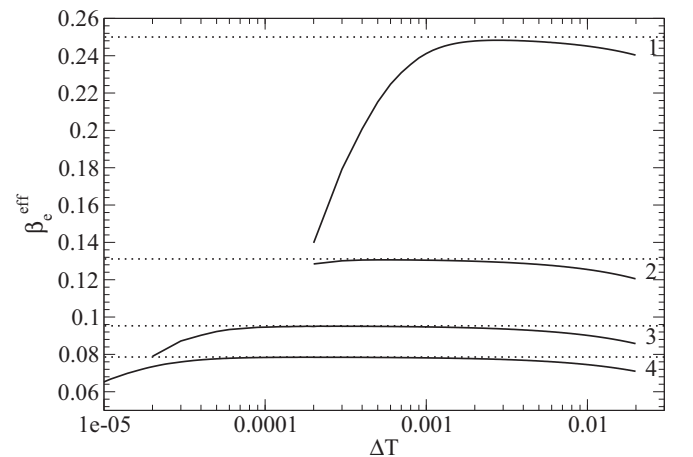FIG. 14. The symmetric eight-vertex model with $c \neq d$: the dependence of β_e^{eff} on ΔT for four choices of the critical vertex weights (4.2). Baxter's exact values are represented by dotted lines.
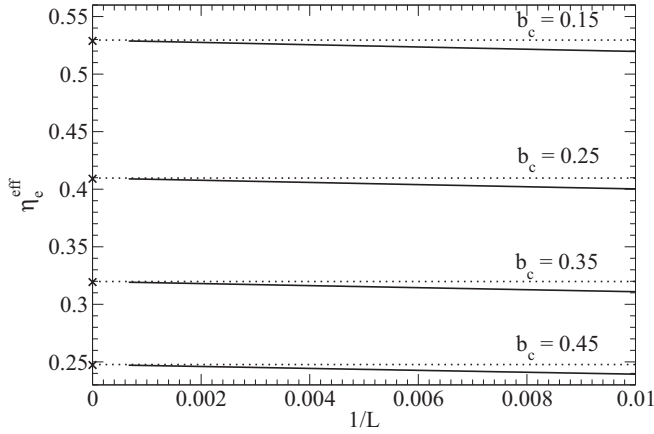
FIG. 15. The symmetric eight-vertex model with $c = d$: the dependence of the effective critical exponent η_e^{eff} on the inverse system size $1/L$, for four values of the critical vertex weight $b_c = 0.15, 0.25, 0.35$, and 0.45. The suggested values obtained from (5.1) are represented by dotted lines.

FIG. 17. The symmetric eight-vertex model with $c = d$: the dependence of the effective critical exponent δ_e^{eff} on the the applied electric field E, for four values of the critical vertex weight $b_c = 0.15, 0.25, 0.35$, and 0.45. The δ_e values are identified with the minimum points of the plots, the suggested values (5.1) are represented by dotted lines.

plots. The δ_e values are identified with the minimum points of the plots, the suggested values (5.1) are represented by dotted lines.

For the vertex weights $c = d$, the dependence of the electric effective central charge c_e^{eff} on the inverse system size $1/L$ is pictured in Fig. 19. As before for the magnetic case, for all four values of the critical vertex weight, $b_c = 0.15, 0.25, 0.35$, and 0.45, the plots tend as $1/L \to 0$ to the same value $c_e = 1$.

Numerical data for the electric exponents obtained from Figs. 13–19 are tabulated in Table II. The comparison with the Baxter's exact result for β_e or the values obtained from our suggested formulas in Eq. (5.1) shows a high precision of our numerical results.
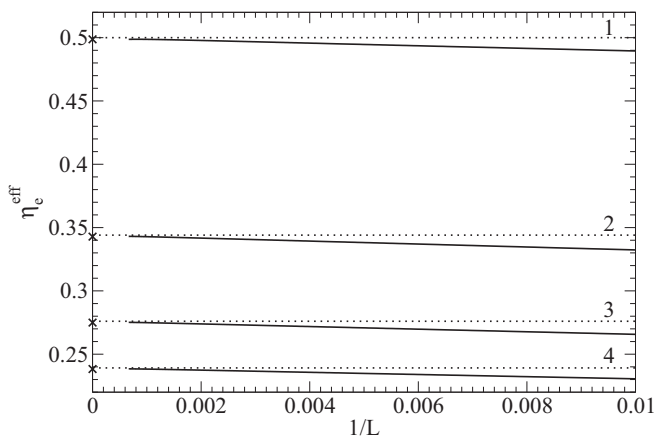
TABLE II. Numerical data for the electric exponents and central charge obtained from Figs. 13–19 and compared with Baxter's exact result for β_e (2.30) or the values generated from our suggested formulas (5.1).

Fig. 13:	$b_c = 0.15$	$\beta_e^{\mathrm{num}} = 0.2801$	$\beta_e^{\mathrm{exact}} = 0.2814$
	$= 0.25$	$= 0.1731$	$= 0.1735$
	$= 0.35$	$= 0.1174$	$= 0.1175$
	$= 0.45$	$= 0.0822$	$= 0.0823$
Fig. 14:	1	$\beta_e^{\mathrm{num}} = 0.2483$	$\beta_e^{\mathrm{exact}} = 0.2500$
	2	$= 0.1306$	$= 0.1311$
	3	$= 0.0951$	$= 0.0953$
	4	$= 0.0785$	$= 0.0786$
Fig. 15:	$b_c = 0.15$	$\eta_e^{\mathrm{num}} = 0.5288$	$\eta_e^{\mathrm{sugg}} = 0.5296$
	$= 0.25$	$= 0.4091$	$= 0.4097$
	$= 0.35$	$= 0.3193$	$= 0.3198$
	$= 0.45$	$= 0.2473$	$= 0.2477$
Fig. 16:	1	$\eta_e^{\mathrm{num}} = 0.4987$	$\eta_e^{\mathrm{sugg}} = 0.5000$
	2	$= 0.3428$	$= 0.3440$
	3	$= 0.2750$	$= 0.2760$
	4	$= 0.2383$	$= 0.2392$
Fig. 17:	$b_c = 0.15$	$\delta_e^{\mathrm{num}} = 6.5561$	$\delta_e^{\mathrm{sugg}} = 6.5539$
	$= 0.25$	$= 8.7674$	$= 8.7641$
	$= 0.35$	$= 11.5123$	$= 11.5077$
	$= 0.45$	$= 15.1562$	$= 15.1500$
Fig. 18:	1	$\delta_e^{\mathrm{num}} = 7.0054$	$\delta_e^{\mathrm{sugg}} = 7.0000$
	2	$= 10.6365$	$= 10.6265$
	3	$= 13.5057$	$= 13.4928$
	4	$= 15.7393$	$= 15.7251$
Fig. 19:	$b_c = 0.15$	$c_e^{\mathrm{num}} = 0.9988$	$c_e^{\mathrm{sugg}} = 1$
	$= 0.25$	$= 0.9987$	$= 1$
	$= 0.35$	$= 0.9985$	$= 1$
	$= 0.45$	$= 0.9985$	$= 1$

FIG. 16. The symmetric eight-vertex model with $c \neq d$: the dependence of η_e^{eff} on $1/L$, for four choices of the critical vertex weights (4.2). The suggested values obtained from (5.1) are represented by dotted lines.
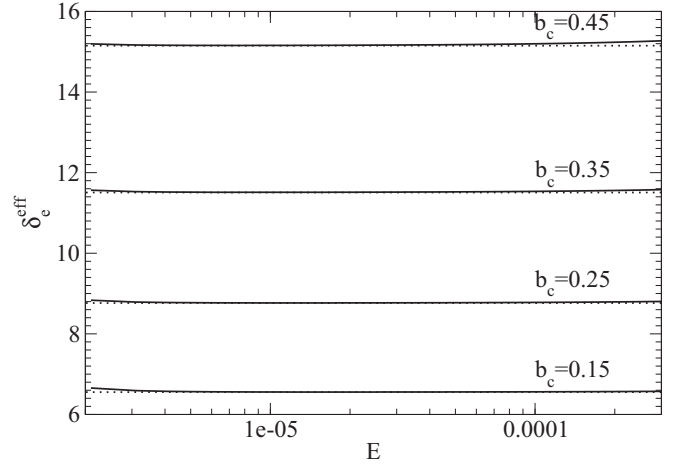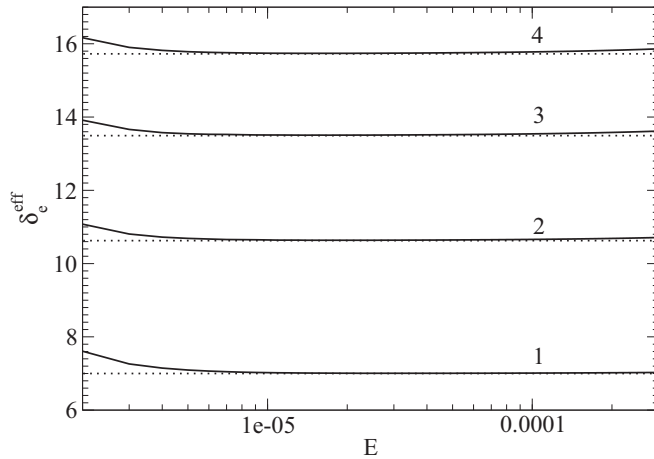
FIG. 18. The symmetric eight-vertex model with $c \neq d$: the dependence of $\delta_{\mathrm{e}}^{\mathrm{eff}}$ on the electric field E for four choices of the critical vertex weights (4.2). The suggested values (5.1) are represented by dotted lines.
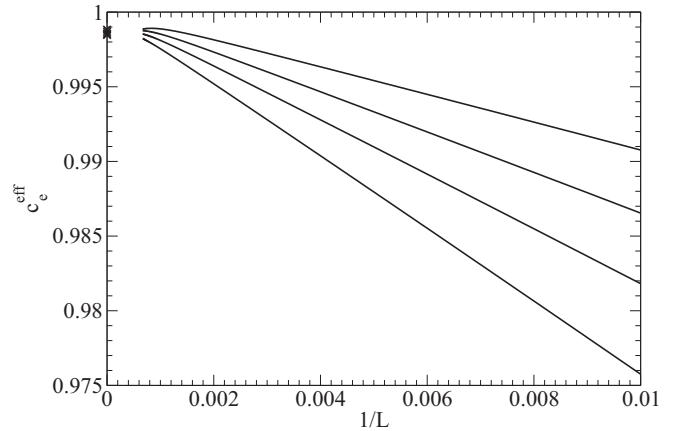

FIG. 19. The symmetric eight-vertex model with $c = d$: the dependence of the effective electric central charge $c_{\mathrm{e}}^{\mathrm{eff}}$ on $1/L$ for four values of the critical vertex weight $b_c = 0.15$, 0.25, 0.35, and 0.45. As $1/L \to 0$, all curves tend to $c_{\mathrm{e}} = 1$.

VI. CONCLUSION

Baxter solved the symmetric eight-vertex model on the square lattice within its magnetic formulation of Ising spins on the dual square lattice with plaquette interactions. Some of the magnetic critical exponents depend on the model's parameters. Pointing out a freedom in the definition of deviation from the critical point, Suzuki proposed a rescaling of critical indices. The rescaled indices become constant, namely 2D Ising-like, and this property is known as weak universality. Weak universality requires that the exponents η and δ, which are defined just at the critical temperature and therefore do not depend on the definition of the deviation from the critical temperature, are constant and indeed $\eta = 1/4$ and $\delta = 15$. We tested our numerical estimates of critical indices against Baxter's exact results (dotted lines) in Figs. 4–11; see also numerical data in Table I—the agreement is very good.

As concerns the original vertex (electric) formulation, Baxter was able to derive the explicit formula (2.30) for the critical exponent β_{e} related to the spontaneous polarization. The crucial point of our analysis was the equivalence of the exponents ν and ν_{e} in Eq. (3.15). Combining this relation with Baxter's exact result for β_{e} (2.30) and the scaling relations

(2.37), the suggested exponents η_{e} and δ_{e} (5.1) turn out to be dependent on the model's parameters. As is seen in Figs. 15 and 16, the numerical check of the suggested formula for η_{e} is very good. The same applies to the numerical checks of the suggested formula for δ_{e}; see Figs. 17 and 18. Since the critical exponents η_{e} and δ_{e} are defined just at the critical temperature and therefore are independent of the definition of the deviation from the critical temperature, their dependence on the model's parameters means that the electric-vertex formulation of the model is fully nonuniversal. Consequently, in spite of the equivalence of the partition functions, the magnetic and electric versions of the model possess different critical properties.

We believe that this work will be a motivation for a rigorous derivation of the suggested formulas (5.1), maybe by using the QISM machinery. The full nonuniversality of statistical models is probably not so exceptional as is generally believed.

[1] B. Sutherland, J. Math. Phys. **11**, 3183 (1970).

[2] C. Fan and F. Y. Wu, Phys. Rev. B **2**, 723 (1970).

[3] R. J. Baxter, Phys. Rev. Lett. **26**, 832 (1971).

[4] R. J. Baxter, Ann. Phys. (NY) **70**, 193 (1972).

[5] R. J. Baxter, Ann. Phys. (NY) **70**, 323 (1972).

[6] R. J. Baxter, *Exactly Solved Models in Statistical Mechanics*, 3rd ed. (Dover, New York, 2007).

[7] E. K. Sklyanin and L. D. Faddeev, Dokl. Acad. Nauk SSSR **243**, 1430 (1978).

[8] E. K. Sklyanin and L. D. Faddeev, Dokl. Acad. Nauk SSSR **244**, 1337 (1978).

[9] V. E. Korepin, N. M. Bogoliubov, and A. G. Izergin, *Quantum Inverse Scattering Method and Correlation Functions* (Cambridge University Press, Cambridge, England, 1993).

[10] L. Šamaj and Z. Bajnok, *Introduction to the Statistical Physics of Integrable Many-body Systems* (Cambridge University Press, Cambridge, England, 2013).

[11] F. Y. Wu, Phys. Rev. B **4**, 2312 (1971).

[12] L. P. Kadanoff and F. J. Wegner, Phys. Rev. B **4**, 3989 (1971).

[13] R. B. Griffiths, Phys. Rev. Lett. **24**, 1479 (1970).

[14] M. Suzuki, Prog. Theor. Phys. **51**, 1992 (1974).

[15] J. M. J. Van Leeuwen, Phys. Rev. Lett. **34**, 1056 (1975).

[16] L. P. Kadanoff and A. C. Brown, Ann. Phys. (NY) **121**, 318 (1979).

[17] H. J. F. Knops, Ann. Phys. (NY) **128**, 448 (1980).

[18] R. Krčmár and L. Šamaj, Europhys. Lett. **115**, 56001 (2016).

[19] J. Ashkin and E. Teller, Phys. Rev. **64**, 178 (1943).

[20] C. Fan, Phys. Lett. A **39**, 136 (1972).

[21] L. P. Kadanoff, Phys. Rev. Lett. **39**, 903 (1977).

[22] A. B. Zisook, J. Phys. A: Math. Gen. **13**, 2451 (1980).

[23] F. Alet, J. L. Jacobsen, G. Misguich, V. Pasquier, F. Mila, and M. Troyer, Phys. Rev. Lett. **94**, 235702 (2005).

[24] S. L. A. de Queiroz, Phys. Rev. E **84**, 031132 (2011).

[25] S. Jin, A. Sen, and A. W. Sandvik, Phys. Rev. Lett. **108**, 045702 (2012).

[26] T. Suzuki, K. Harada, H. Matsuo, S. Todo, and N. Kawashima, Phys. Rev. B **91**, 094414 (2015).

[27] R. F. S. Andrade and H. J. Herrmann, Phys. Rev. E **88**, 042122 (2013).

[28] M. Kolesík and L. Šamaj, J. Stat. Phys. **72**, 1203 (1993).

[29] M. Kolesík and L. Šamaj, Phys. Lett. A **177**, 87 (1993).

[30] L. Bernardi and I. A. Campbell, Phys. Rev. B **52**, 12501 (1995).

[31] S. Bekhechi and B. W. Southern, Phys. Rev. B **67**, 144403 (2003).

[32] A. Omerzu, M. Tokumoto, B. Tadić, and D. Mihailovic, Phys. Rev. Lett. **87**, 177205 (2001).

[33] F. Kagawa, K. Miyagawa, and K. Kanoda, Nature (London) **436**, 534 (2005).

[34] P. Kulish and E. Sklyanin, Zap. Nauchn. Sem. LOMI **95**, 129 (1980); J. Soviet. Math. **19**, 1596 (1982).

[35] J. T. Chalker and P. D. Coddington, J. Phys. C: Solid State Phys. **21**, 2665 (1988).

[36] D.-H. Lee, Phys. Rev. B **50**, 10788 (1994).

[37] J. Kondev and J. B. Marston, Nucl. Phys. B **497**, 639 (1997).

[38] P. Fendley, B. Nienhuis, and K. Schoutens, J. Phys. A: Math. Gen. **36**, 12399 (2003).

[39] Ch. Hagendorf and P. Fendley, J. Stat. Phys. **146**, 1122 (2012).

[40] J. de Gier and P. Pyatov, J. Stat. Mech. (2004) P002.

[41] A. Nichols, V. Rittenberg, and J. de Gier, J. Stat. Mech. (2005) P03003.

[42] P. Zinn-Justin, *Six-vertex, Loop and Tilling Models: Integrability and Combinatorics* (Lambert Academic Publishing, 2010).

[43] C. M. Fortuin and P. W. Kasteleyn, Physica **57**, 536 (1972).

[44] C. M. Fortuin, Physica **58**, 393 (1972); **59**, 545 (1972).

[45] G. Grimmett, *The Random-Cluster Model*, Grundlehren der Mathematischen Wissenschaften Vol. 333 (Springer-Verlag, Berlin, 2006).

[46] V. Pasquier, Nucl. Phys. B **285**, 162 (1987); J. Phys. A: Math. Gen. **20**, 5707 (1987).

[47] A. L. Owczarek and R. J. Baxter, J. Stat. Phys. **49**, 1093 (1987).

[48] F. Y. Wu, Rev. Mod. Phys. **54**, 235 (1982).

[49] J. L. Jacobsen and H. Saleur, Nucl. Phys. B **743**, 207 (2006).

[50] H. N. V. Temperley and E. H. Lieb, Proc. R. Soc. London, Ser. A **322**, 251 (1971).

[51] J. D. Johnson and S. Krinsky, Phys. Rev. A **8**, 2526 (1973).

[52] A. Luther and I. Peschel, Phys. Rev. B **12**, 3908 (1975).

[53] A. Takada and K. Kubo, J. Phys. Soc. Jpn. **55**, 1671 (1986).

[54] K. Kubo, T. A. Kaplan, and J. R. Borysowicz, Phys. Rev. B **38**, 11550 (1988).

[55] S. Liang, Phys. Rev. Lett. **64**, 1597 (1990).

[56] H. Q. Lin and D. K. Campbell, J. Appl. Phys. **69**, 5947 (1991).

[57] K. A. Hallberg, P. Horsch, and G. Martínez, Phys. Rev. B **52**, R719 (1995).

[58] S. R. White, Phys. Rev. Lett. **69**, 2863 (1992).

[59] S. R. White, Phys. Rev. B **48**, 10345 (1993).

[60] U. Schollwöck, Rev. Mod. Phys. **77**, 259 (2005).

[61] R. Krčmár and L. Šamaj, Phys. Rev. E **92**, 052103 (2015).

[62] P. Calabrese and J. Cardy, J. Stat. Mech. (2004) P06002.

[63] E. Ercolessi, S. Evangelisti, and F. Ravanini, Phys. Lett. A **374**, 2101 (2010).

[64] T. Nishino and K. Okunishi, J. Phys. Soc. Jpn. **65**, 891 (1996).

[65] T. Nishino and K. Okunishi, J. Phys. Soc. Jpn. **66**, 3040 (1997).

[66] E. Carlon, M. Henkel, and U. Schollwoeck, Eur. Phys. J. **B12**, 99 (1999).

[67] T. Nishino, K. Okunishi, and M. Kikuchi, Phys. Lett. A **213**, 69 (1996).